Trabecular Bone Score (TBS)—A Novel Method to Evaluate Bone Microarchitectural Texture in Patients With Primary Hyperparathyroidism

Barbara Campolina Silva, Stephanie Boutroy, Chiyuan Zhang, Donald Jay McMahon, Bin Zhou, Ji Wang, Julia Udesky, Serge Cremers, Marta Sarquis, Xiang-Dong Edward Guo, Didier Hans, and John Paul Bilezikian

Metabolic Bone Diseases Unit (B.C.S., S.B., C.Z., D.J.M., J.U., S.C., J.P.B.), Division of Endocrinology, Department of Medicine, College of Physicians and Surgeons, and Bone Bioengineering Laboratory (B.Z., J.W., X.E.G.), Department of Biomedical Engineering, Columbia University, New York, New York 10032; College of Medicine (B.C.S., M.S.), Federal University of Minas Gerais, Belo Horizonte 31270-901, Brazil; Institut National de la Santé et de la Recherche Médicale U1033 and University of Lyon (S.B.), 69003 Lyon, France; and Center of Bone Diseases (D.H.), Lausanne University Hospital, 1011 Lausanne, Switzerland

Context: In the milder form of primary hyperparathyroidism (PHPT), cancellous bone, represented by areal bone mineral density at the lumbar spine by dual-energy x-ray absorptiometry (DXA), is preserved. This finding is in contrast to high-resolution peripheral quantitative computed tomography (HRpQCT) results of abnormal trabecular microstructure and epidemiological evidence for increased overall fracture risk in PHPT. Because DXA does not directly measure trabecular bone and HRpQCT is not widely available, we used trabecular bone score (TBS), a novel gray-level textural analysis applied to spine DXA images, to estimate indirectly trabecular microarchitecture.

Objective: The purpose of this study was to assess TBS from spine DXA images in relation to HRpQCT indices and bone stiffness in radius and tibia in PHPT.

Design and Setting: This was a cross-sectional study conducted in a referral center.

Patients: Participants were 22 postmenopausal women with PHPT.

Main Outcome Measures: Outcomes measured were areal bone mineral density by DXA, TBS indices derived from DXA images, HRpQCT standard measures, and bone stiffness assessed by finite element analysis at distal radius and tibia.

Results: TBS in PHPT was low at 1.24, representing abnormal trabecular microstructure (normal $\geq$1.35). TBS was correlated with whole bone stiffness and all HRpQCT indices, except for trabecular thickness and trabecular stiffness at the radius. At the tibia, correlations were observed between TBS and volumetric densities, cortical thickness, trabecular bone volume, and whole bone stiffness. TBS correlated with all indices of trabecular microarchitecture, except trabecular thickness, after adjustment for body weight.

Conclusion: TBS, a measurement technology readily available by DXA, shows promise in the clinical assessment of trabecular microstructure in PHPT. **(*J Clin Endocrinol Metab* 98: 1963–1970, 2013)**

Abbreviations: 2D, two-dimensional; 3D, three-dimensional; aBMD, areal bone mineral density; BSAP, bone-specific alkaline phosphatase; BV/TV, trabecular bone volume; Ct.Th, cortical thickness; Ct.vBMD, cortical volumetric bone density; CTX, C-teleopeptide; CUMC, Columbia University Medical Center; DXA, dual-energy x-ray absorptiometry; FEA, finite element analysis; HRpQCT, high-resolution peripheral quantitative computed tomography; μCT, microcomputed tomography; OC, osteocalcin; PHPT, primary hyperparathyroidism; Tb.N, trabecular number; TBS, trabecular bone score; Tb.Sp, trabecular separation; Tb.Sp.SD, standard deviation of trabecular separation; Tb.Th, trabecular thickness; Tb.vBMD, trabecular volumetric bone density; UD, ultradistal; vBMD, volumetric bone mineral density.

ISSN Print 0021-972X ISSN Online 1945-7197
Printed in U.S.A.

Received December 19, 2012. Accepted February 20, 2013.
First Published Online April 22, 2013

Primary hyperparathyroidism (PHPT) is a common endocrine disorder characterized by hypercalcemia and elevated or inappropriately normal levels of PTH. With the advent of the multichannel autoanalyzer in the early 1970s, the clinical presentation of PHPT changed from symptomatic (1) to asymptomatic (2–4). Whereas overt skeletal disease, formerly a common finding, is rarely seen now, dual-energy X-ray absorptiometry (DXA) routinely detects evidence for skeletal involvement. The distal one-third radius, a dominant site of cortical bone, is typically more involved than the lumbar spine, a site of predominantly trabecular bone (5). These findings, however, are not consistent with recent observations using technologies that have greater resolving power than DXA, such as high-resolution peripheral quantitative computed tomography (HRpQCT) in which trabecular microarchitectural deficits are seen (6, 7). By HRpQCT, both trabecular and cortical compartments are abnormal at the radius and tibia in postmenopausal women with PHPT. These deficits are associated with reduced whole bone and trabecular stiffness by finite element analysis (FEA) (7). Hansen et al (6) have also observed similar structural deficits at the distal radius in PHPT. These more recent findings by HRpQCT and FEA are consistent with epidemiological evidence of increased fracture risk at both vertebral and nonvertebral sites in PHPT (8–11). Whereas HRpQCT has added a dimension of insight not previously seen with regard to trabecular bone in PHPT, HRpQCT is not widely available and remains so far a research tool.

Trabecular bone score (TBS) is a novel gray-level textural analysis that can be applied to DXA images to estimate trabecular microarchitecture and has been shown to be related to direct measures of bone microarchitecture and fracture risk (12). Using experimental variograms of two-dimensional (2D) projection images, TBS differentiates between three-dimensional (3D) bone structures that exhibit the same areal bone mineral density (aBMD), but different trabecular microarchitecture (13). TBS analysis is readily available from the lumbar spine DXA image without the need for further imaging or expensive instrumentation. Studies in cadaveric bones have shown significant correlations between TBS and 3D trabecular microarchitecture measurements by microcomputed tomography (μCT) (12–14). In clinical studies, TBS enhanced the ability of DXA to predict fracture risk (15–20), and in a recent study involving more than 29,000 postmenopausal women, TBS predicted osteoporotic fractures, independent of aBMD (20). Finally, Boutroy et al (21) showed that TBS predicts osteoporotic fracture as well as lumbar spine aBMD and that TBS helps to define a subset of nonosteoporotic women at high risk for fracture.

The ability of TBS to estimate trabecular microarchitectural texture and predict fracture risk, along with its direct measurement from DXA images, led us to investigate its potential utility in evaluating the trabecular skeleton in PHPT. To this end, our aim was to assess TBS from spine DXA images in postmenopausal women with PHPT and to correlate it, for the first time, with HRpQCT measurements of volumetric bone density, skeletal microarchitecture, and bone stiffness.

Patients and Methods

Study subjects

Twenty-two postmenopausal women with PHPT were recruited from Columbia University Medical Center (CUMC). Subjects were eligible for inclusion if they had well-characterized PHPT (elevated serum calcium and elevated or inappropriately normal PTH levels). Exclusion criteria included bisphosphonate or glucocorticoid use within the past 2 years, a history of Cushing syndrome, uncontrolled thyroid disease, malabsorption syndrome, significant liver disease, creatinine clearance <30 mL/min, and any chronic disorders of mineral metabolism such as Paget disease or osteogenesis imperfecta. Women were considered postmenopausal if they had not had a menstrual period for more than 1 year. Among the 29 women screened, 1 was excluded because of her premenopausal status and 6 were excluded because of a history of bisphosphonate use within 2 years before study.

The study was approved by the institutional review board of CUMC, and all subjects gave written informed consent.

DXA

aBMD by DXA was measured at the lumbar spine (L1–L4), total hip, femoral neck, and nondominant forearm (ultradistal [UD] radius and one-third radius) using a Discovery A dual-energy X-ray absorptiometer (Hologic Inc; Bedford, Massachusetts). Bone mineral density was expressed in grams per square centimeter and in T-score unitage.

TBS

Site-matched spine TBS parameters were extracted from the DXA image using TBS iNsight software (version 1.9; medimaps, Geneva, Switzerland). TBS measurements were performed in the Bone Disease Unit at the University of Lausanne (Lausanne, Switzerland), using deidentified spine DXA files from scans obtained at CUMC. TBS was evaluated by determining the variogram of the trabecular bone projected image, calculated as the sum of the squared gray-level differences between pixels at a specific distance and angle. TBS was then calculated as the slope of the log-log transform of this variogram (13). The mean value of the individual measurements for L1–L4 represents the lumbar spine TBS (unitless).

To ensure comparability with previous TBS studies, calibration of the DXA instrument at CUMC was performed using a TBS-specific phantom (medimaps). With use of an extensively calibrated dataset based on more than 35,000 women, normal and abnormal scores have been established: TBS ≤ 1.2 defines degraded microarchitecture, TBS between 1.20 and 1.35 is par-

tially degraded microarchitecture, and TBS ≥1.35 is considered normal (19–23).

HRpQCT

Volumetric bone mineral density (vBMD) and microarchitecture were measured at the nondominant distal radius and tibia using the HRpQCT system (voxel size 82 μm, XtremeCT; Scanco Medical AG, Brüttisellen, Switzerland) at CUMC, as described previously (24).

Image analysis has been validated and detailed elsewhere (24–27). The following indices were evaluated at the distal radius and tibia: total area and total vBMD, cortical vBMD (Ct.vBMD), and trabecular vBMD (Tb.vBMD); cortical thickness (Ct.Th); trabecular bone volume (BV/TV); trabecular number (Tb.N); trabecular thickness (Tb.Th); trabecular separation (Tb.Sp); and standard deviation of trabecular separation (Tb.Sp.SD), a parameter reflecting the heterogeneity of the trabecular network.

FEA of HRpQCT images

FEA was performed to estimate whole bone and trabecular stiffness by converting whole bone and trabecular HRpQCT images into finite element models. For each finite element model, a uniaxial compression test was performed with displacement equivalent to 1% apparent strain to calculate stiffness. Bone tissue was assumed to have an isotropic linear material property with a Young modulus of 15 GPa and a Poisson ratio of 0.3. Whole bone stiffness was defined as the reaction force divided by the applied displacement. This measurement characterizes the mechanical competence of both cortical and trabecular compartments, and it is closely related to whole bone strength (28). Likewise, trabecular bone stiffness characterizes the mechanical competence of the trabecular bone compartment.

Biochemical analysis

Serum total calcium (normal, 8.4–10.2 mg/dL) and albumin were measured using standard methods (Quest Diagnostics, Madison, New Jersey), and calcium values were corrected for albumin concentration <4 g/dL. Intact PTH (normal, 14–66 pg/mL) was measured by immunoradiometric assay (Scantibodies Laboratory, Santee, California) in the Bone Marker Laboratory at CUMC. The inter- and intra-assay coefficients are <7% and <5%, respectively. Serum intact amino-terminal propeptide of type I procollagen (Orion Diagnostica, Espoo, Finland) was measured by radioimmunoassay (normal, 19–83 μg/L). Serum N-Mid osteocalcin (OC) (IDS, Scottsdale, Arizona), bone-specific alkaline phosphatase (BSAP) (Quidel, San Diego, California), and C-telopeptide (CTX) (IDS) were measured by ELISA. The reference ranges in premenopausal women for OC, BSAP, and CTX were, respectively, 8.4 to 33.9 ng/mL, 11.6 to 29.6 U/L, and 0.112 to 0.738 ng/mL.

Statistical analysis

Descriptive statistics are expressed as means ± SEM. The correlation of TBS with HRpQCT indices, mechanical parameters, and DXA measurements was assessed by the Pearson correlation test. Because Tb.Sp and Tb.Sp.SD did not follow a normal distribution, they were log-transformed before analysis. Linear regression analyses, without and with adjustment for weight, were applied to estimate the variability in HRpQCT and biomechanical parameters when TBS, aBMD at the lumbar spine, or the combination of both was used as the explanatory variable. All statistical tests were performed at the 2-sided $P < .05$ significance level. Statistical analysis was performed using SAS (version 9.2; SAS Institute, Inc, Cary, North Carolina).

Table 1. Baseline Characteristics of 22 Subjects With PHPT

Characteristics	PHPT (n = 22)
Age, y	67 ± 2
Weight, kg	71 ± 4
Height, cm	161.5 ± 1.9
BMI, kg/cm^2	27.2 ± 1.5
Time since menopause, y	15 ± 2
Time since diagnosis, y	6 ± 1
Serum total calcium, mg/dL	10.4 ± 0.1
PTH, pg/mL	72 ± 9
TBS	1.24 ± 0.03
L1–L4 aBMD, g/cm^2	0.940 ± 0.039
T-score	−1.0 ± 0.4
Total hip aBMD, g/cm^2	0.808 ± 0.035
T-score	−1.1 ± 0.3
Femoral neck aBMD, g/cm^2	0.693 ± 0.030
T-score	−1.4 ± 0.3
One-third radius aBMD, g/cm^2	0.616 ± 0.022
T-score	−1.3 ± 0.4
UD radius aBMD, g/cm^2	0.361 ± 0.018
T-score	−1.4 ± 0.3

Data are means ± SEM. The normal range for serum calcium is 8.6 to 10.2 mg/dL and for serum PTH is 14 to 66 pg/mL.

Results

Baseline characteristics of 22 postmenopausal women with PHPT are described in Table 1. Most patients with PHPT (77%) were asymptomatic. Only 1 subject had a history of nephrolithiasis, whereas 4 had a history of fragility fracture. Bone turnover markers (amino-terminal propeptide of type I procollagen, OC, and CTX) were at the upper range of normal, whereas serum BSAP was frankly elevated at 37.6 U/L (normal, 11.6–29.6 U/L). The average creatinine clearance was normal at 77.7 mL/min per 1.73 m^2.

TBS and aBMD by DXA

Mean TBS, aBMD, and T-scores by DXA are shown in Table 1. Although the prevalence of osteoporosis at any site was 50%, the L1–L4 T-score by DXA was well above the WHO osteoporosis threshold (T-score ≤2.5) in the vast majority of subjects. Only 3 (14%) patients were classified as osteoporotic and 7 (32%) as osteopenic, whereas the remaining 12 (54%) subjects presented with normal L1–L4 T-scores by DXA. In marked contrast, TBS at the lumbar spine showed degraded microarchitecture (TBS ≤1.20) in 8 (36%) patients, partially degraded (TBS >1.20 and <1.35) in an additional 8 patients (36%), and

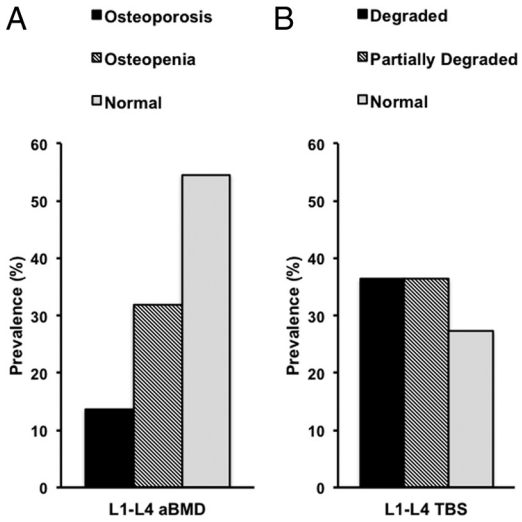

Figure 1. Prevalence of subjects with osteoporosis, osteopenia, or normal aBMD at the lumbar spine by DXA (A) and degraded microarchitecture (TBS ≤1.2), partially degraded microarchitecture (TBS >1.2 and <1.35), and normal TBS at the lumbar spine (TBS ≥1.35) (B).

normal values (TBS ≥ 1.35) in only 6 (27%) subjects (Figure 1, A and B). The mean TBS of the whole group was 1.24, markedly below the normal threshold (≥1.35).

Relationship between TBS and aBMD by DXA

Correlations between TBS and aBMD at the lumbar spine ($r = 0.367$), total hip ($r = 0.269$), and femoral neck ($r = 0.350$) were not significant, but significant correlations were found between TBS and aBMD at the one-third radius ($r = 0.427$; $P = .047$) and UD radius ($r = 0.450$; $P = .036$).

Relationship between TBS, HRpQCT, and mechanical parameters

As shown in Table 2, TBS was significantly correlated with all radius HRpQCT and biomechanical measurements except total area, Tb.Th, and trabecular stiffness. Significant correlations remained after adjustment for body weight (Table 2 and Figure 2).

TBS was significantly correlated with tibia HRpQCT with regard to volumetric densities, Ct.Th, BV/TV, and whole bone stiffness. All indices of trabecular microarchitecture, except Tb.Th, became significant after adjusting for body weight (Table 2 and Figure 2).

With the use of linear regression analysis, TBS or L1–L4 aBMD alone explained 20 to 52% of variance in HRpQCT measurements of volumetric densities, Ct.Th, BV/TV, and whole bone stiffness at the radius and tibia. TBS and aBMD together better predicted the variability in these HRpQCT indices and whole bone stiffness than either one alone (Table 3).

At the radius, TBS explained 25% and 21% of the variance in Tb.N and Tb.Sp, respectively, with a slight increase in the degree of variance explained by the combination of TBS with L1–L4 aBMD compared with L1–L4 aBMD alone (Table 3). At the tibia, TBS was a poor predictor of the variance in HRpQCT measurements of trabecular microarchitecture.

The addition of weight in the model increased the total variance in HRpQCT measurements, and TBS was no longer distinctly associated with HRpQCT indices when body weight was included in the analyses.

Table 2. Correlation Between TBS and HRpQCT/Mechanical Parameters at the Radius and at the Tibia in Subjects With PHPT (n = 22)

	TBS	
	r Value	*r* Value Adjusted for Weight
Radius		
Total area	−0.153	−0.063
Total vBMD	0.489[a]	0.536[a]
Ct.vBMD	0.507[a]	0.512[a]
Ct.Th	0.453[a]	0.480[a]
Tb.vBMD	0.476[a]	0.562[a]
BV/TV	0.473[a]	0.559[a]
Tb.N	0.505[a]	0.620[a]
Tb.Th	0.317	0.337
Tb.Sp (log)	−0.492[a]	−0.580[a]
Tb.Sp.SD (log)	−0.441[a]	−0.533[a]
Trabecular stiffness	0.332	0.326
Whole bone stiffness	0.442[a]	0.530[a]
Tibia		
Total area	−0.373	−0.259
Total vBMD	0.619[a]	0.668[a]
Ct.vBMD	0.471[a]	0.465[a]
Ct.Th	0.515[a]	0.545[a]
Tb.vBMD	0.528[a]	0.606[a]
BV/TV	0.530[a]	0.608[a]
Tb.N	0.297	0.573[a]
Tb.Th	0.056	−0.112
Tb.Sp (log)	−0.365	−0.524[a]
Tb.Sp.SD (log)	−0.390	−0.483[a]
Trabecular stiffness	0.262	0.403
Whole bone stiffness	0.516[a]	0.609[a]

[a] $P < .05$.

Discussion

The results of this study show, for the first time, significant correlations between TBS and HRpQCT measurements of volumetric densities, skeletal microarchitecture, and bone stiffness at the radius and tibia in a group of postmenopausal women with PHPT. Previous HRpQCT studies have shown that not only cortical but also trabecular bone is compromised in PHPT, even in the mild form of this disease (6, 7). This technology, however, is not widely accessible, and a clinical tool to assess trabecular microarchitecture could be helpful in the evaluation of this

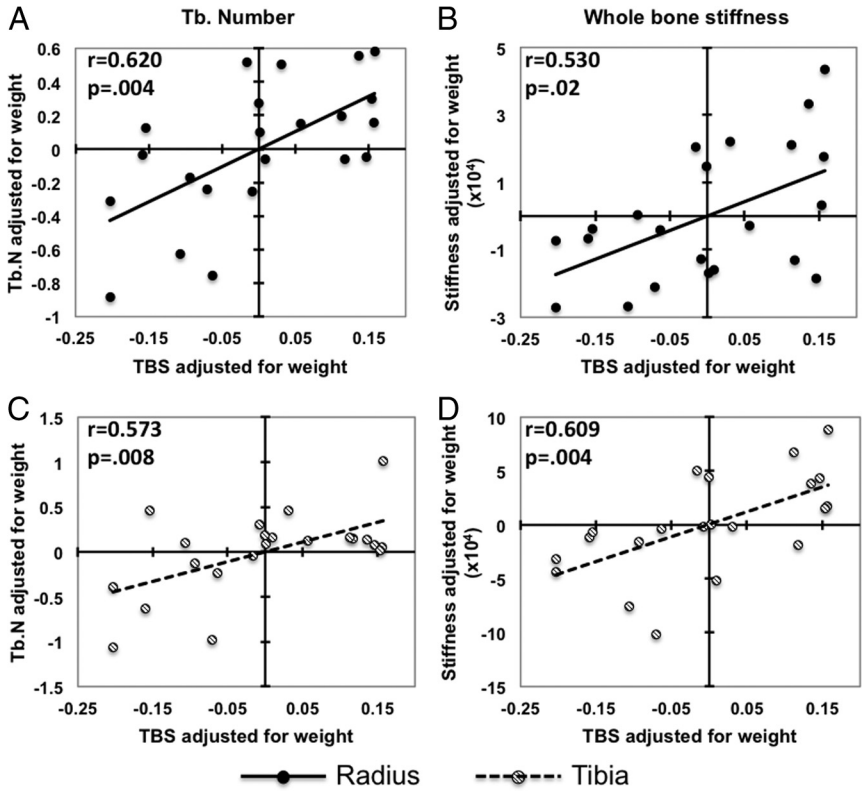

Figure 2. Correlations adjusted for body weight between TBS and trabecular number (A and C) and whole bone stiffness (B and D) at the radius/tibia.

disease. TBS, an indirect measurement of trabecular microarchitecture, is now an US Food and Drug Administration–approved application applied to DXA images and is readily available. Significant correlations between TBS and HRpQCT indices demonstrated here indicate that TBS may serve as a valuable additional index in the assessment of skeletal microstructure in PHPT.

Significant correlations between TBS and 3D direct measurements of trabecular microstructure were previously observed in human cadaver bone specimens (vertebrae, femur, and radius) (12, 13). The pivotal TBS study showed significant relationships between TBS evaluated from 2D projection images directly derived from 3D μCT reconstruction and direct 3D measurements of trabecular microarchitecture by μCT (12). After this observation, TBS was derived from DXA images of lumbar vertebrae, and significant correlations between trabecular indices by μCT and TBS were confirmed (13, 14). In agreement with these data, we observed a positive correlation between TBS and BV/TV and Tb.N and a negative correlation with Tb.Sp and Tb.Sp.SD at the radius. At the tibia, correlations between TBS and Tb.N, Tb.Sp, or Tb.Sp.SD became significant only after adjustment for body weight, a surrogate for biomechanical loading. Although the lumbar spine and tibia are both load-bearing sites, they are subjected to different loading forces, which might explain this observation. Differences in the quality of trabecular bone can also be recognized when HRpQCT findings are compared with histomorphometric and μCT analyses of iliac crest bone biopsy samples in PHPT. Although both cortical and trabecular bone are abnormal when assessed by HRpQCT at the radius and tibia, histomorphometry and μCT studies of iliac crest biopsy samples show that trabecular bone volume, number, separation, and connectivity are either preserved or increased in PHPT (29–33). Cohen et al (34) have also found modest or no correlations between microarchitecture parameters as assessed by HRpQCT of the radius and tibia and histomorphometry and μCT of iliac crest biopsy samples. Because previous studies have shown strong correlations between microarchitecture assessed by HRpQCT and histomorphometry or μCT at the same bony regions (25, 35), site-to-site differences are likely to contribute to the weak correlations observed by Cohen et al (34). The discrepant observations by histomorphometric analysis of bone biopsy samples vis-à-vis fracture incidence in this disease suggest that HRpQCT and now TBS might be more clinically pertinent to fracture risk in PHPT.

Despite the fact that TBS estimates trabecular microarchitecture, our results also revealed positive correlations between TBS and Ct.vBMD and Ct.Th at the radius and tibia. This finding is not surprising, because cortical and trabecular compartments are both affected in PHPT, leading to strong correlations between measurements of trabecular and cortical microarchitecture and density, even among HRpQCT indices (eg, correlation between Tb.N and Ct.Th at the radius: $r = 0.667$; $P = .001$). Moreover, because TBS is assessed on 2D projection images, it is not likely that TBS analyzes purely trabecular bone.

Using linear regression analysis, variations in HRpQCT measurements of volumetric density were better predicted by the combination of TBS and L1–L4 aBMD than by either one alone. However, HRpQCT indices of trabecular microarchitecture and stiffness were better predicted by L1–L4 aBMD, and the combination of TBS and L1–L4 aBMD was only slightly better in predicting their variance. Likewise, although our results showed positive relationships between TBS and whole bone stiffness at the radius and tibia, no significant correlations between TBS

Table 3. Univariate or Multivariate Linear Regression Analysis to Predict the Variability in HRpQCT Indices and Mechanical Parameters

		aBMD (R^2)	
	TBS (R^2)	L1–L4	TBS + L1–L4
Radius			
Total area	0.023	0.004	0.039
Total vBMD	0.239[a]	0.330[a]	0.420[a]
Ct.vBMD	0.257[a]	0.209[a]	0.342[a]
Ct.Th	0.205[a]	0.233[a]	0.321[a]
Tb.vBMD	0.227[a]	0.479[a]	0.536[a]
BV/TV	0.224[a]	0.479[a]	0.534[a]
Tb.N	0.255[a]	0.460[a]	0.536[a]
Tb.Th	0.100	0.269[a]	0.287[a]
Tb.Sp	0.208[a]	0.345[a]	0.411[a]
Tb.Sp.SD	0.161	0.315[a]	0.359[a]
Trabecular stiffness	0.110	0.365[a]	0.379[a]
Whole bone stiffness	0.195[a]	0.522[a]	0.558[a]
Tibia			
Total area	0.139	0.004	0.187
Total vBMD	0.383[a]	0.369[a]	0.550[a]
Ct.vBMD	0.222[a]	0.209[a]	0.315[a]
Ct.Th	0.265[a]	0.276[a]	0.396[a]
Tb.vBMD	0.278[a]	0.345[a]	0.458[a]
BV/TV	0.280[a]	0.345[a]	0.459[a]
Tb.N	0.088	0.642[a]	0.642[a]
Tb.Th	0.003	0.184[a]	0.237
Tb.Sp	0.127	0.343[a]	0.366[a]
Tb.Sp.SD	0.123	0.277[a]	0.306[a]
Trabecular stiffness	0.069	0.123	0.141
Whole bone stiffness	0.266[a]	0.444[a]	0.518[a]

[a] $P < .05$.

and trabecular stiffness were observed either at the radius or at the tibia, even after adjustment for body weight. Because trabecular microstructure can differ significantly among different anatomical sites, it is possible that these weak relationships are explained by the comparison of a method that estimates trabecular microarchitecture at the lumbar spine (TBS) with a technology that measures trabecular microstructure and stiffness at the radius and tibia (HRpQCT). In fact, when TBS, aBMD, and measurements of trabecular microstructure by μCT were assessed at the same bony region, correlations of aBMD and TBS with BV/TV, Tb.N, Tb.Sp, and connectivity density were similar (13). Likewise, a recent ex vivo study on 16 human vertebrae showed a positive relationship between TBS assessed in L3 and mechanically measured bone stiffness of the same vertebra (14).

The amount of variance in HRpQCT indices explained by TBS and weight was greater than that for TBS alone. Because of the increase in variance due to the addition of weight as a variable, TBS lost its predictive value. Because BMI is taken into account in the calculation of the TBS, part of the variability in HRpQCT measurements explained by TBS alone might depend on some interaction of TBS with weight.

Although we have not assessed differences in TBS in patients with PHPT with or without fracture, we did show positive correlations between TBS and whole bone stiffness at the radius ($r = 0.442$; $P = .04$) and at the tibia ($r = 0.516$; $P = .02$) as measured by FEA of HRpQCT images. Reduced bone stiffness assessed by FEA of HRpQCT images (36, 37), as well as low TBS (15–17, 19–21), has been associated with fragility fractures in postmenopausal women. In addition to predicting fracture risk in primary osteoporosis and healthy subjects, TBS has also been shown to predict fracture in individuals with secondary osteoporosis related to several diseases, such as diabetes, rheumatoid arthritis, and subclinical hypercortisolism (38–40). Even though these studies did not involve patients with PHPT, our findings suggest that low TBS may be related with decreased bone stiffness, and consequently, fracture risk, also in PHPT.

As reported previously (22, 41), we observed modest or no correlation between TBS and aBMD at all sites. Weak relationships of TBS with aBMD at the lumbar spine, femoral neck, and total hip were also reported in The Manitoba Study (20). The poor correlation between TBS and aBMD at the lumbar spine, despite the fact that both evaluate the same region of bone, implies that these measurements are at least partially independent of each other. In contrast, Boutroy et al (21) found significant correlations between TBS and L1–L4 aBMD ($r = 0.58$; $P < .001$) in 560 women from the OFELY cohort. However, part of this correlation was partially confounded with age. Nevertheless, there may be a tendency for higher correlations between these 2 indices when Hologic scanners (21, 42) as opposed to GE Lunar DXA devices (20, 43) are used. The reason for these discrepant findings is still not clear but is probably related to the image resolution, the DXA soft tissue correction applied, and the spectra of X-ray energies used.

A TBS threshold of 1.200 has been used in numerous studies to identify patients at high risk of fracture. Results from these studies have shown that a significantly greater number of postmenopausal women at high risk of fragility fracture are identified when a combination of either aBMD T-score $\leq$2.5 or TBS $<$1.200 is considered as opposed to aBMD T-score $\leq$2.5 alone (19, 22, 23). Similarly, in the study of Boutroy et al (21), nonosteoporotic women whose TBS values were less than 1.209 (the first TBS quartile threshold) had a significant higher incidence of fragility fracture. Using cutoff points previously reported as having the best sensitivity and specificity in terms of fracture risk (19–23), we showed that 36% of patients with PHPT had degraded microarchitecture (TBS $\leq$1.20), an additional 36% had partially degraded microarchitecture (TBS $>$1.20 and $<$1.35), and only 27% had normal TBS

values (TBS ≥1.35). In contrast to 72% of patients with PHPT showing degraded or partially degraded microarchitecture by TBS, only 46% were classified as osteopenic or osteoporotic by lumbar spine T-score. Likewise, Romagnoli et al (42) recently showed that TBS values were lower in subjects with mild PHPT than in aged-matched healthy control subjects, despite similar lumbar spine aBMDs by DXA (42). Noteworthy conclusions of this study of postmenopausal women with PHPT, therefore, are that TBS may help to identify structural abnormalities in trabecular bone and that conventional DXA assessment is insufficient for this purpose.

This study has limitations. Because of the relatively small number of subjects, we could not evaluate any association between TBS and fracture risk in PHPT. These results also need to be followed up with a larger number of patients along with 2 groups of hyperparathyroid subjects we have yet to study, namely men and premenopausal women. Although we did not have a healthy control group, there is robust experience with normative datasets that have already defined normal values for this technology.

Our study has important strengths. This is the first clinical study to report significant correlations between TBS and direct measurements of trabecular microstructure by HRpQCT. The positive relationship between TBS and whole bone stiffness assessed by FEA of HRpQCT images suggests that, in PHPT, low TBS may also indicate increased fracture risk. Moreover, our results demonstrate that TBS has the potential to identify subjects with PHPT with abnormalities in trabecular bone not captured by lumbar spine aBMD. TBS has the major clinical advantage of being readily available from images of DXA, a test routinely performed in PHPT. With significant correlations between TBS and volumetric and microstructural indices, as well as biomechanical measurements by HRpQCT, a method that has greater resolving power but is not widely accessible, TBS could become a helpful clinical tool in the assessment of skeletal involvement in PHPT.

Acknowledgments

Address all correspondence and requests for reprints to: John P. Bilezikian, MD, College of Physicians and Surgeons, 630 West 168 Street, New York, New York 10032 E-mail: jpb2@columbia.edu; or Barbara C. Silva, 630 West 168 Street, New York, New York 10032. E-mail: bcs2131@columbia.edu.

This work was supported by the National Institutes of Health (Grants R01 DK32333 and R01 AR051376) and by the Brazilian National Council of Technological and Scientific Development (to B.C.S.).

Disclosure Summary: D.H. is a co-owner of the patent for TBS. The other authors have nothing to disclose.

References

1. **Cope O.** The study of hyperparathyroidism at the Massachusetts General Hospital. *N Engl J Med*. 1966;274:1174–1182.
2. **Rubin MR, Bilezikian JP, McMahon DJ, et al.** The natural history of primary hyperparathyroidism with or without parathyroid surgery after 15 years. *J Clin Endocrinol Metab*. 2008;93:3462–3470.
3. **Silverberg SJ, Shane E, Jacobs TP, Siris E, Bilezikian JP.** A 10-year prospective study of primary hyperparathyroidism with or without parathyroid surgery. *N Engl J Med*. 1999;341:1249–1255.
4. **Bilezikian JP, Brandi ML, Rubin M, Silverberg SJ.** Primary hyperparathyroidism: new concepts in clinical, densitometric and biochemical features. *J Intern Med*. 2005;257:6–17.
5. **Silverberg SJ, Shane E, de la Cruz L, et al.** Skeletal disease in primary hyperparathyroidism. *J Bone Miner Res*. 1989;4:283–291.
6. **Hansen S, Beck Jensen JE, et al.** Effects on bone geometry, density, and microarchitecture in the distal radius but not the tibia in women with primary hyperparathyroidism: A case-control study using HR-pQCT. *J Bone Miner Res*. 2010;25:1941–1947.
7. **Stein EM, Silva BC, Boutroy S, et al.** Primary hyperparathyroidism is associated with abnormal cortical and trabecular microstructure and reduced bone stiffness in postmenopausal women. *J Bone Miner Res*. 2012 Dec 7. doi: 10.1002/jbmr. 1841.
8. **Khosla S, Melton LJ 3rd, Wermers RA, Crowson CS, O'Fallon W, Riggs B.** Primary hyperparathyroidism and the risk of fracture: a population-based study. *J Bone Miner Res*. 1999;14:1700–1707.
9. **Vignali E, Viccica G, Diacinti D, et al.** Morphometric vertebral fractures in postmenopausal women with primary hyperparathyroidism. *J Clin Endocrinol Metab*. 2009;94:2306–2312.
10. **Yu N, Donnan PT, Flynn RW, Murphy MJ, Smith D, Rudman A, Leese GP.** Increased mortality and morbidity in mild primary hyperparathyroid patients. The Parathyroid Epidemiology and Audit Research Study (PEARS). *Clin Endocrinol (Oxf)*. 2010;73:30–34.
11. **Vestergaard P, Mosekilde L.** Fractures in patients with primary hyperparathyroidism: nationwide follow-up study of 1201 patients. *World J. Surg*. 2003;27:343–349.
12. **Pothuaud L, Carceller P, Hans D.** Correlations between grey-level variations in 2D projection images (TBS) and 3D microarchitecture: applications in the study of human trabecular bone microarchitecture. *Bone*. 2008;42:775–787.
13. **Hans D, Barthe N, Boutroy S, Pothuaud L, Winzenrieth R, Krieg MA.** Correlations between trabecular bone score, measured using anteroposterior dual-energy X-ray absorptiometry acquisition, and 3-dimensional parameters of bone microarchitecture: an experimental study on human cadaver vertebrae. *J Clin Densitom*. 2011; 14:302–312.
14. **Roux JP, Wegrzyn J, Boutroy S, Bouxsein M, Hans D, Chapurlat R.** The predictive value of trabecular bone score (TBS) on whole lumbar vertebrae mechanics: an ex-vivo study [published online March 2013]. *Osteoporos Int*. doi:10.1007/s00198-013-2316-7.
15. **Pothuaud L, Barthe N, Krieg MA, Mehsen N, Carceller P, Hans D.** Evaluation of the potential use of trabecular bone score to complement bone mineral density in the diagnosis of osteoporosis: a preliminary spine BMD-matched, case-control study. *J Clin Densitom*. 2009;12:170–176.
16. **Rabier B, Heraud A, Grand-Lenoir C, Winzenrieth R, Hans D.** A multicentre, retrospective case-control study assessing the role of trabecular bone score (TBS) in menopausal Caucasian women with low areal bone mineral density (BMDa): analysing the odds of vertebral fracture. *Bone*. 2010;46:176–181.
17. **Winzenrieth R, Dufour R, Pothuaud L, Hans D.** A retrospective case-control study assessing the role of trabecular bone score in

postmenopausal Caucasian women with osteopenia: analyzing the odds of vertebral fracture. *Calcif Tissue Int*. 2010;86:104–109.
18. **Del Rio LM, Winzenrieth R, Cormier C, Di Gregorio S.** Is bone microarchitecture status of the lumbar spine assessed by TBS related to femoral neck fracture? A Spanish case-control study. *Osteoporos Int*. 2012;24:991–998.
19. **Popp A, Meer S, Krieg MA, Perrelet R, Hans D, Lippuner K.** Bone mineral density (BMD) combined with the trabecular bone score (TBS) significantly improves the identification of women at high risk of fracture: the SEMOF Cohort Study [abstract]. *J Bone Miner Res*. 2012;27(suppl 1):S303.
20. **Hans D, Goertzen AL, Krieg MA, Leslie WD.** Bone microarchitecture assessed by TBS predicts osteoporotic fractures independent of bone density: the Manitoba study. *J Bone Mineral Res*. 2011;26: 2762–2769.
21. **Boutroy S, Hans D, Sornay-Rendu E, Vilayphiou N, Winzenrieth R, Chapurlat R.** Trabecular bone score improves fracture risk prediction in non-osteoporotic women: the OFELY study. *Osteoporos Int*. 2013;24:77–85.
22. **Lamy O, Krieg MA, Stoll D, Aubry-Rozier B, Metzger M, Hans D.** What is the performance in vertebral fracture discrimination by bone mineral density (BMD), micro-architecture estimation (TBS), body mass index (BMI) and FRAX in stand-alone or combined approaches: The OsteoLaus Study [abstract]. *J Bone Miner Res*. 2012; 27(suppl 1):S236.
23. **Vasic J, Gojkovic F, Petranova T, et al.** Spine micro-architecture estimation (TBS) discriminates major osteoporotic fracture from controls equally well than site matched BMD and independently: the Eastern Europe TBS study [abstract]. *Osteoporos Int*. 2012; 23(suppl 2):S327.
24. **Boutroy S, Bouxsein ML, Munoz F, Delmas PD.** In vivo assessment of trabecular bone microarchitecture by high-resolution peripheral quantitative computed tomography. *J Clin Endocrinol Metab*. 2005;90:6508–6515.
25. **Boutroy S, Vilayphiou N, Roux JP, et al.** Comparison of 2D and 3D bone microarchitecture evaluation at the femoral neck, among postmenopausal women with hip fracture or hip osteoarthritis. *Bone*. 2011;49:1055–1061.
26. **Khosla S, Riggs BL, Atkinson EJ, et al.** Effects of sex and age on bone microstructure at the ultradistal radius: a population-based noninvasive in vivo assessment. *J Bone Miner Res*. 2006;21:124–131.
27. **Liu XS, Zhang XH, Sekhon KK, et al.** High-resolution peripheral quantitative computed tomography can assess microstructural and mechanical properties of human distal tibial bone. *J Bone Miner Res*. 2010;25:746–756.
28. **Macneil JA, Boyd SK.** Bone strength at the distal radius can be estimated from high-resolution peripheral quantitative computed tomography and the finite element method. *Bone*. 2008;42:1203–1213.
29. **Christiansen P, Steiniche T, Vesterby A, Mosekilde L, Hessov I, Melsen F.** Primary hyperparathyroidism: iliac crest trabecular bone volume, structure, remodeling, and balance evaluated by histomorphometric methods. *Bone*. 1992;13:41–49.
30. **Dempster DW, Muller R, Zhou H, et al.** Preserved three-dimensional cancellous bone structure in mild primary hyperparathyroidism. *Bone*. 2007;41:19–24.
31. **Parisien M, Cosman F, Mellish RW, et al.** Bone structure in postmenopausal hyperparathyroid, osteoporotic, and normal women. *J Bone Miner Res*. 1995;10:1393–1399.
32. **Parisien M, Mellish RW, Silverberg SJ, et al.** Maintenance of cancellous bone connectivity in primary hyperparathyroidism: trabecular strut analysis. *J Bone Miner Res*. 1992;7:913–919.
33. **Parisien M, Silverberg SJ, Shane E, et al.** The histomorphometry of bone in primary hyperparathyroidism: preservation of cancellous bone structure. *J Clin Endocrinol Metab*. 1990;70:930–938.
34. **Cohen A, Dempster DW, Muller R, et al.** Assessment of trabecular and cortical architecture and mechanical competence of bone by high-resolution peripheral computed tomography: comparison with transiliac bone biopsy. *Osteoporos Int*. 2010;21:263–273.
35. **MacNeil JA, Boyd SK.** Accuracy of high-resolution peripheral quantitative computed tomography for measurement of bone quality. *Med Eng Phys*. 2007;29:1096–1105.
36. **Boutroy S, Van Rietbergen B, Sornay-Rendu E, Munoz F, Bouxsein ML, Delmas PD.** Finite element analysis based on in vivo HR-pQCT images of the distal radius is associated with wrist fracture in postmenopausal women. *J Bone Miner Res*. 2008;23:392–399.
37. **Stein EM, Liu XS, Nickolas TL, et al.** Abnormal microarchitecture and reduced stiffness at the radius and tibia in postmenopausal women with fractures. *J Bone Miner Res*. 2010;25:2572–2581.
38. **Breban S, Briot K, Kolta S, et al.** Identification of rheumatoid arthritis patients with vertebral fractures using bone mineral density and trabecular bone score. *J Clim Densitom*. 2012;15:260–266.
39. **Leslie WD, Aubry-Rozier B, Lamy O, Hans D.** TBS (trabecular bone score) and diabetes-related fracture risk. *J Clin Endocrinol Metab*. 2013;98:602–609.
40. **Eller-Vainicher C, Morelli V, Ulivieri FM, et al.** Bone quality, as measured by trabecular bone score in patients with adrenal incidentalomas with and without subclinical hypercortisolism. *J Bone Miner Res*. 2012;27:2223–2230.
41. **Popp AW, Guler S, Lamy O, et al.** Effects of zoledronate versus placebo on spine bone mineral density (BMD) and microarchitecture assessed by the trabecular bone score (TBS) in postmenopausal women with osteoporosis. A 3-year study. *J Bone Miner Res*. 2013; 28:449–454.
42. **Romagnoli E, Cipriani C, Nofroni I, et al.** Trabecular bone score (TBS): an indirect measure of bone micro-architecture in postmenopausal patients with primary hyperparathyroidism. *Bone*. 2013;53: 154–159.
43. **Krieg MA, Aubry-Rozier B, Hans D, Leslie WD.** Effects of antiresorptive agents on trabecular bone score (TBS) in older women. *Osteoporos Int* 2013;24:1073–1078.